Supporting Information

Characterization of reversibly switchable fluorescent proteins (rsFPs) in optoacoustic imaging

Paul Vetschera[a,b,+], Kanuj Mishra[a,+], Juan Pablo Fuenzalida-Werner[a], Andriy Chmyrov[a,c], Vasilis Ntziachristos[a,b,c] and Andre C. Stiel[a,*]

[a]) Institute of Biological and Medical Imaging (IBMI), Helmholtz Zentrum München, Neuherberg, Germany
[b]) Chair of Biological Imaging, Technische Universität München, Munich, Germany
[c]) Center for Translational Cancer Research (TranslaTUM), München, Germany
[+]) These authors contributed equally
*) Correspondence should be addressed to A.C.S. (andre.stiel@helmholtz-muenchen.de)

Contents

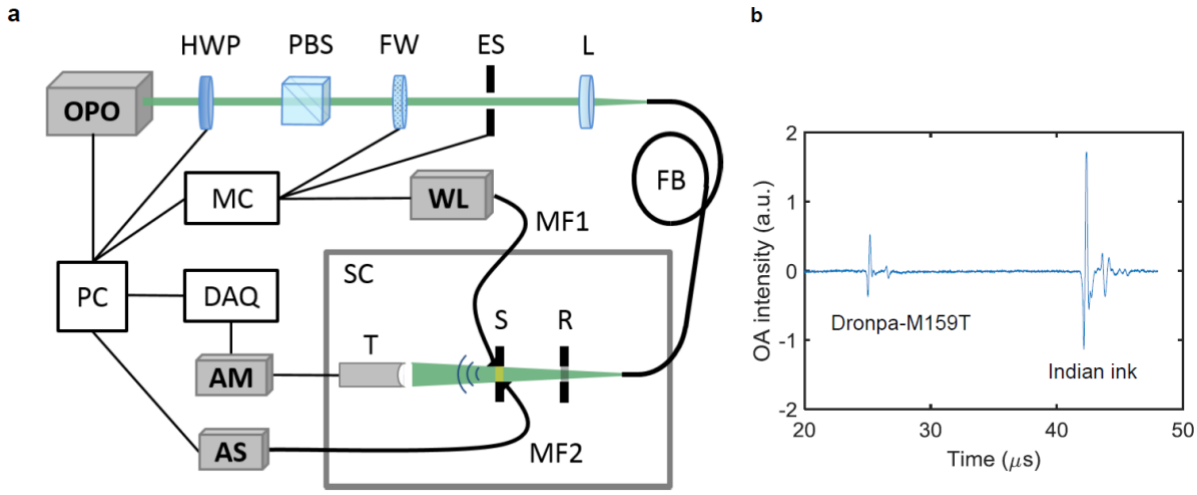

Figure S1. Multimodal Optoacoustic and Absorbance spectrometer used in this study. Abbreviations in **a**: OPO: Optical Parametric Oscillator, HWP, Half waveplate, PBS: Polarizing beam splitter, FW: Filter wheel, ES: Electronic shutter, L: Lens, FB: Fiber bundle, WL: Whitelight lamp, MF: Multimode fiber, AS: Absorption spectrometer, SC: Sample chamber, R: Reference chip, S: Sample chip, T: Transducer, AM: Amplifier, DAQ: Data acquisition card, MC: Microcontroller, PC: Personal Computer. Panel **b** shows a typical averaged time transient (N=10) for Dronpa-M159T at 485nm excitation with the 1st peak being the protein Dronpa-M159T and the 2nd peak being indian ink as the reference signal.

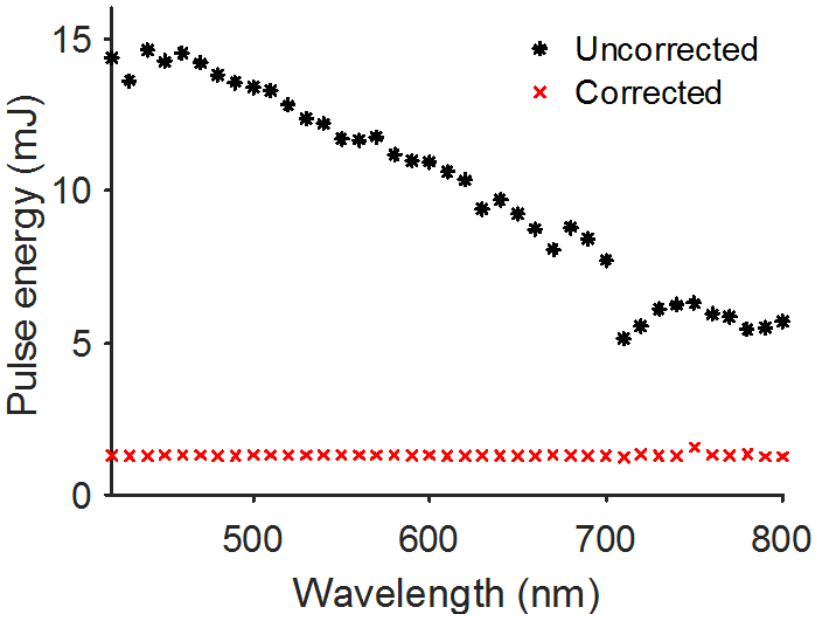

Figure S2 Uncorrected and Corrected energy spectrum for the laser source used throughout the experiments. Laser pulse energy measured at the output of the fiber bundle uncorrected (black stars) or after the power correction using a halfwave-plate and a polarizing beam splitter (red crosses, see supplementary figure 1).

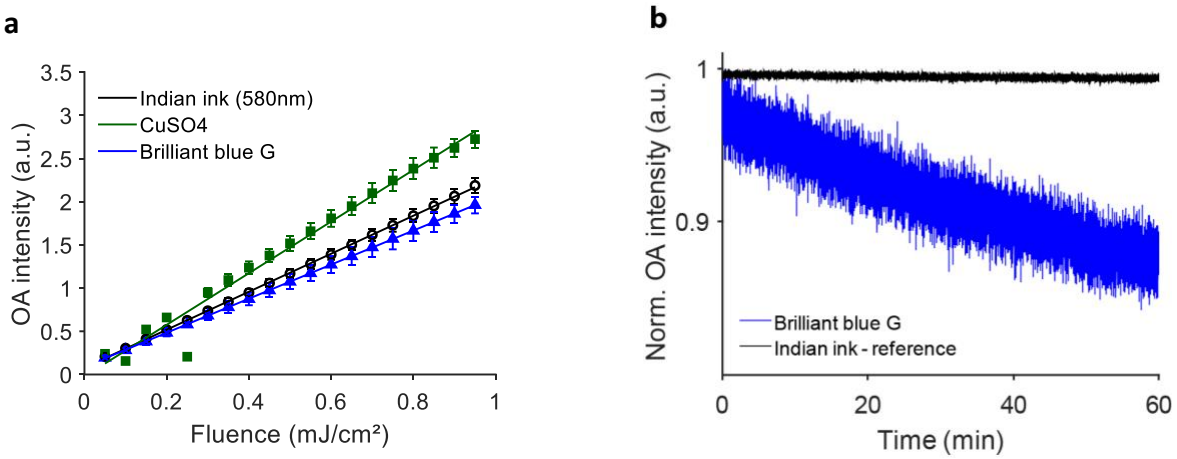

Figure S3. Linearity (a) and stability (b) of optoacoustic reference compounds under laser illuminations used in the experiments. All samples are measured in the sample-position of the spectrometer. Error bars are given for n=3 measurements.

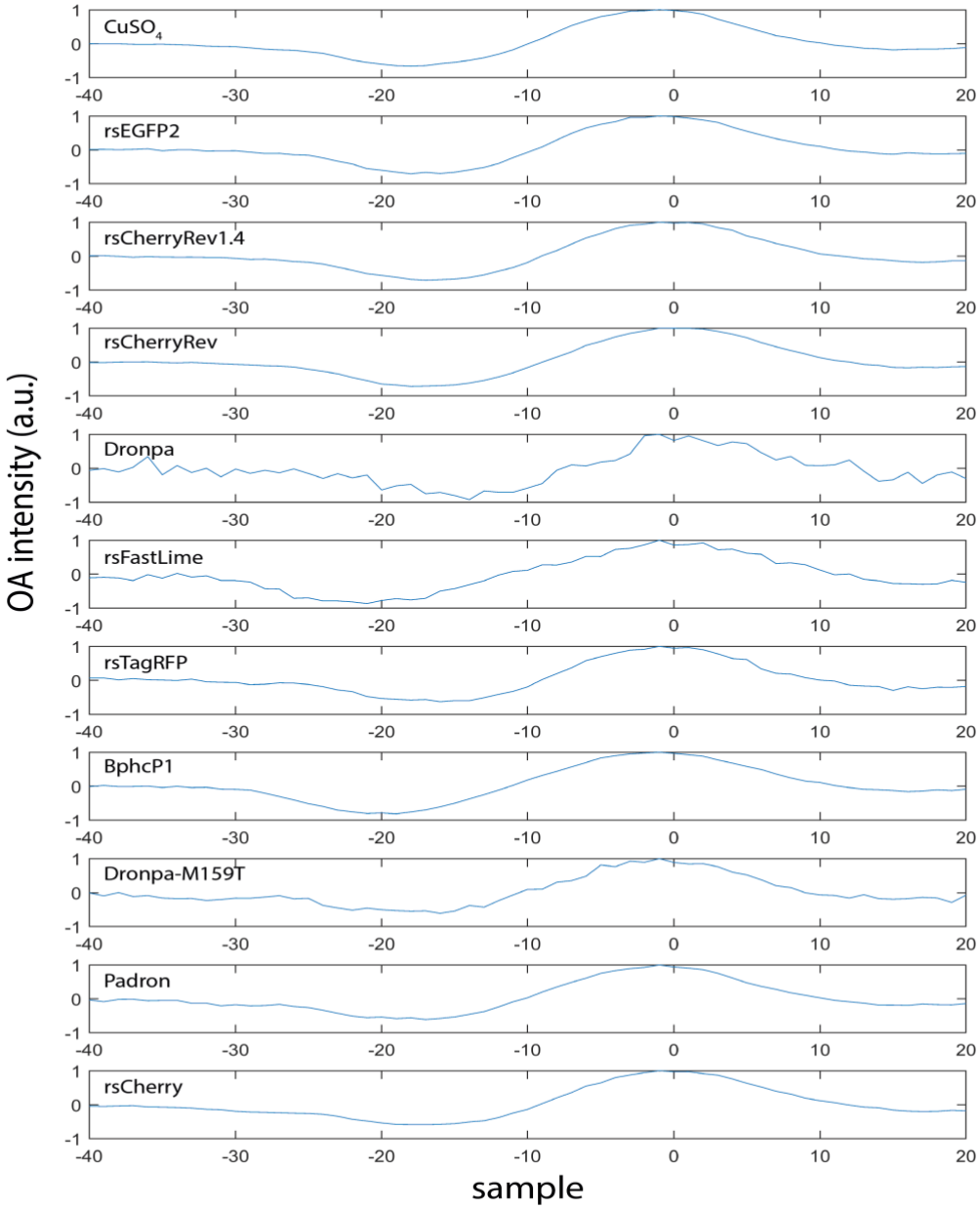

Figure S4. Exemplary optoacoustic waveforms of the reference and samples used in this study. Sampling frequency was 100 MS/s. To ease comparison signals have been normalized to their maximum amplitude as well as to their position in respect to the in-line reference (Indian-ink, see methods for details).

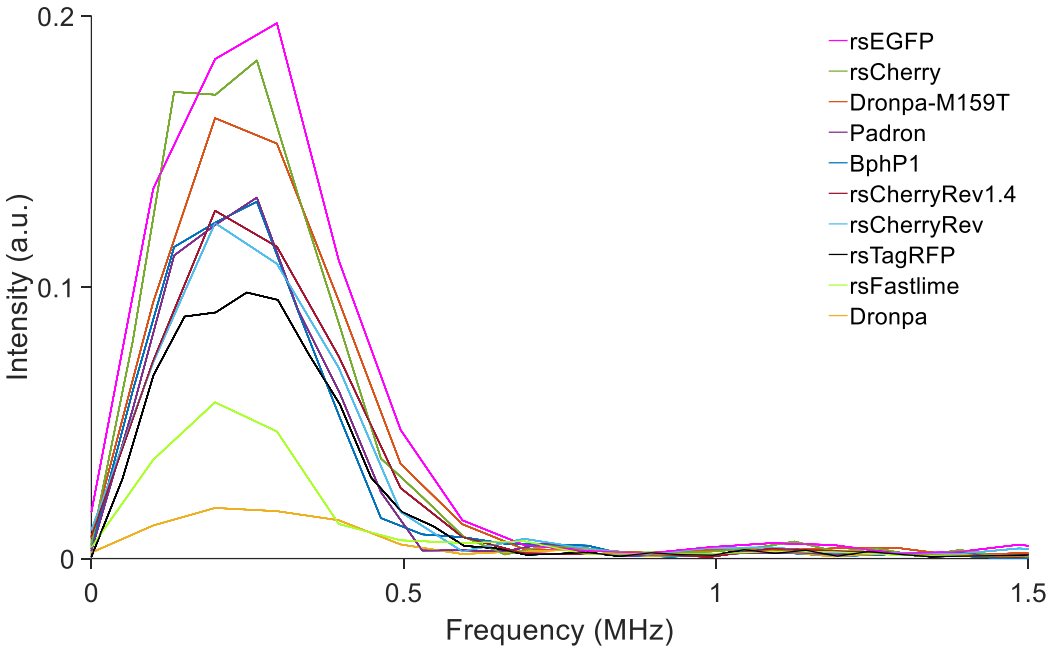

Figure S5. Frequency content of the peak signal of the spectra in Figure 2 (ON-state) after fast-Fourier transformation (FFT).

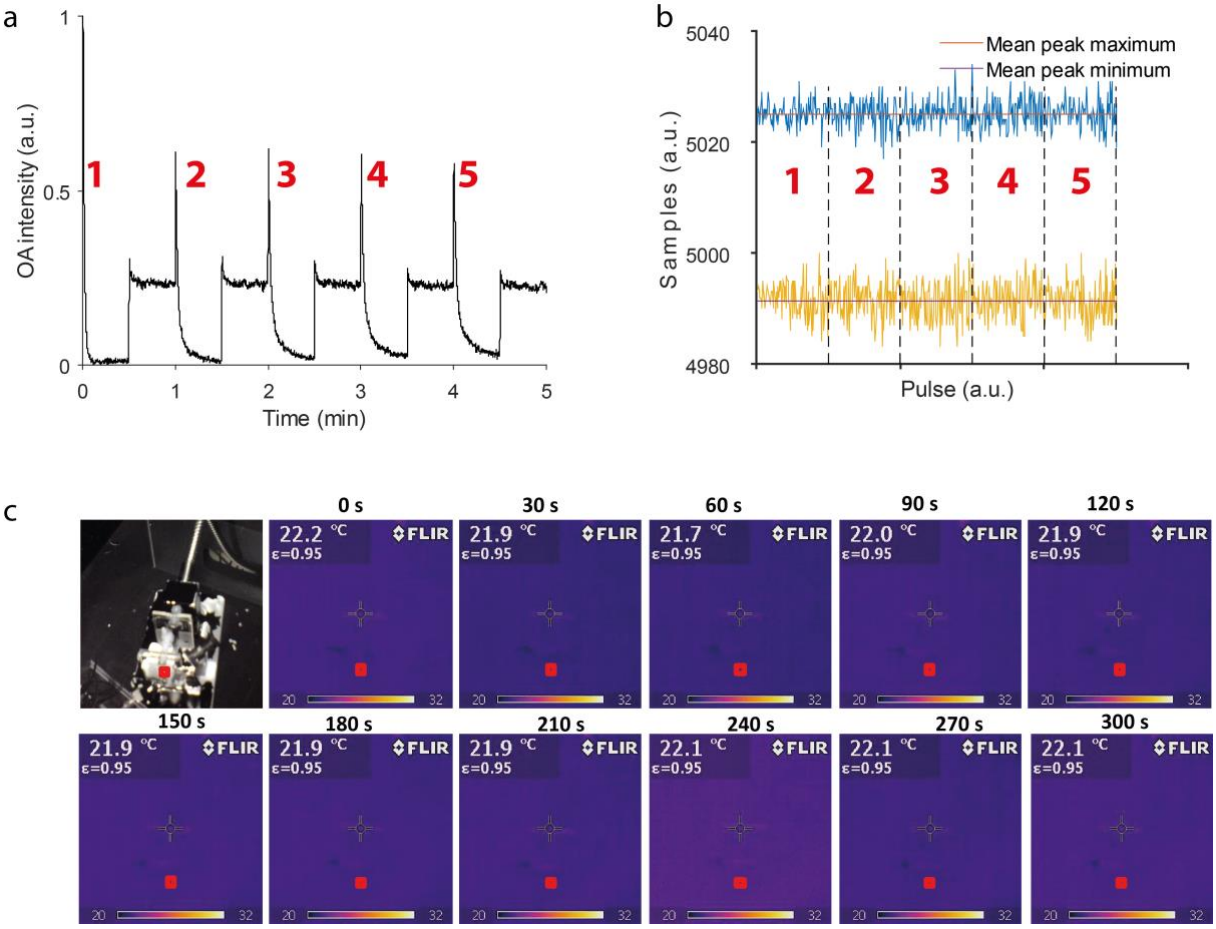

Figure S6. Monitoring of the temperature within the sample chamber. a) Change of optoacoustic signal of upon switching with light at 488 and 420nm. b) Position of the maximum and minimum peaks of the optoacoustic signal (in Samples) for the first 100 pulses of each of the 5 cycles recorded in the experiment shown in a. c) Temperature in the sample chamber during measurements for the experiment shown in A. The temperature indicated in the upper left corner is an average of the measured temperatures in the red square which indicated the position of the sample chamber (FLIR E60, FLIR Systems GmbH, Germany, better than 0.05°C sensitivity).

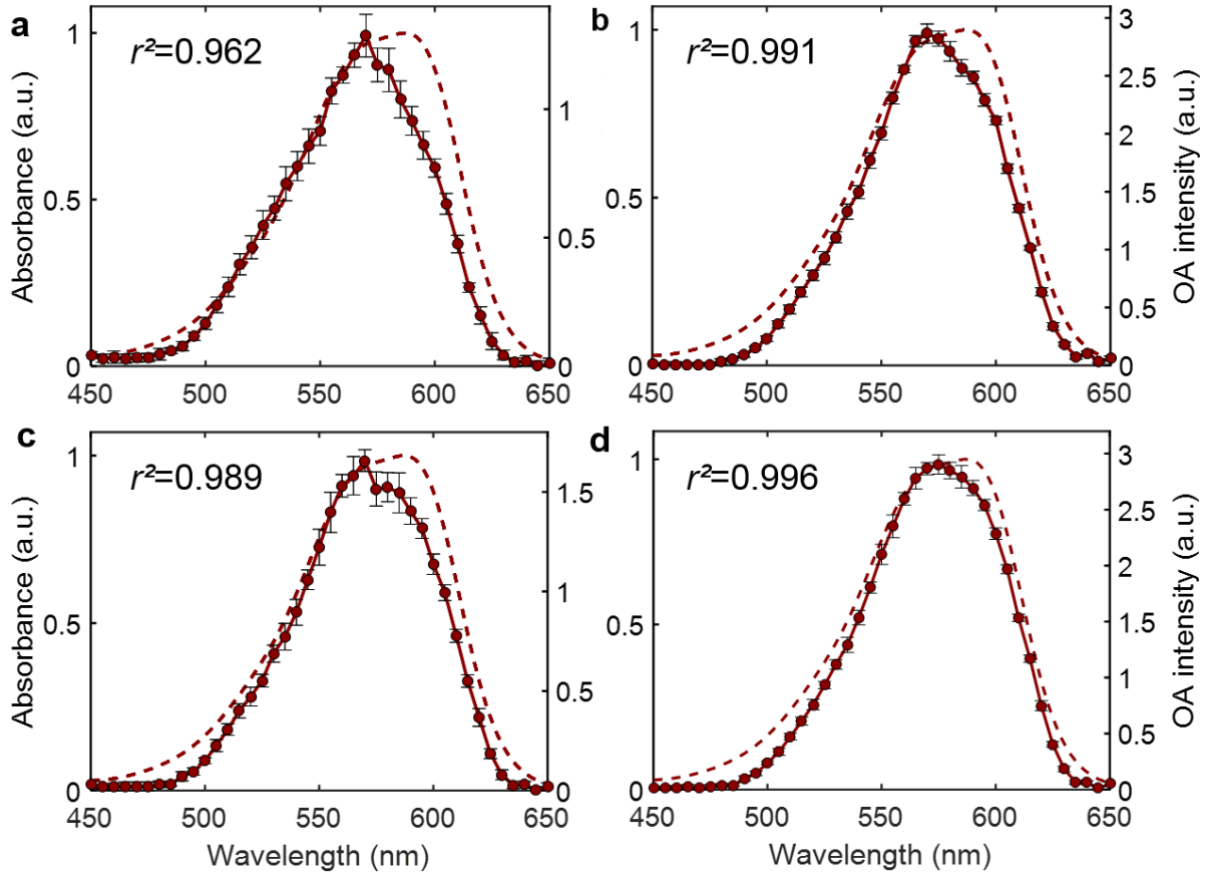

Figure S7. Improvement of Optoacoustic spectra quality**.** Optoacoustic (solid) and absorbance (thin / hollow) spectra of HcRed. a) No power correction, no ink correction, b) No power correction, ink correction, c) power correction, no ink correction, d) power correction, ink correction. r^2 denotes the correlation coefficient of the optoacoustic and the absorbance spectra.

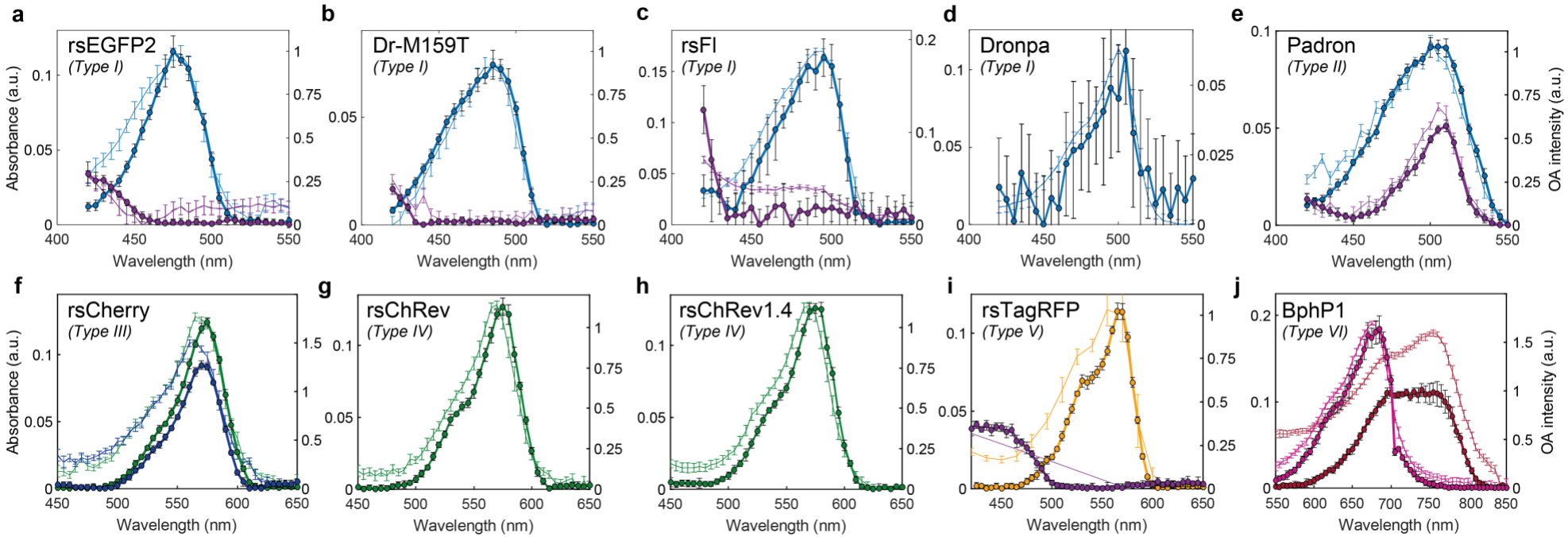

Figure S8. Optoacoustic (solid) and absorbance (thin / hollow) spectra of rsFPs in both switched states recorded concomitantly. Results are presented as described in Figure 2.

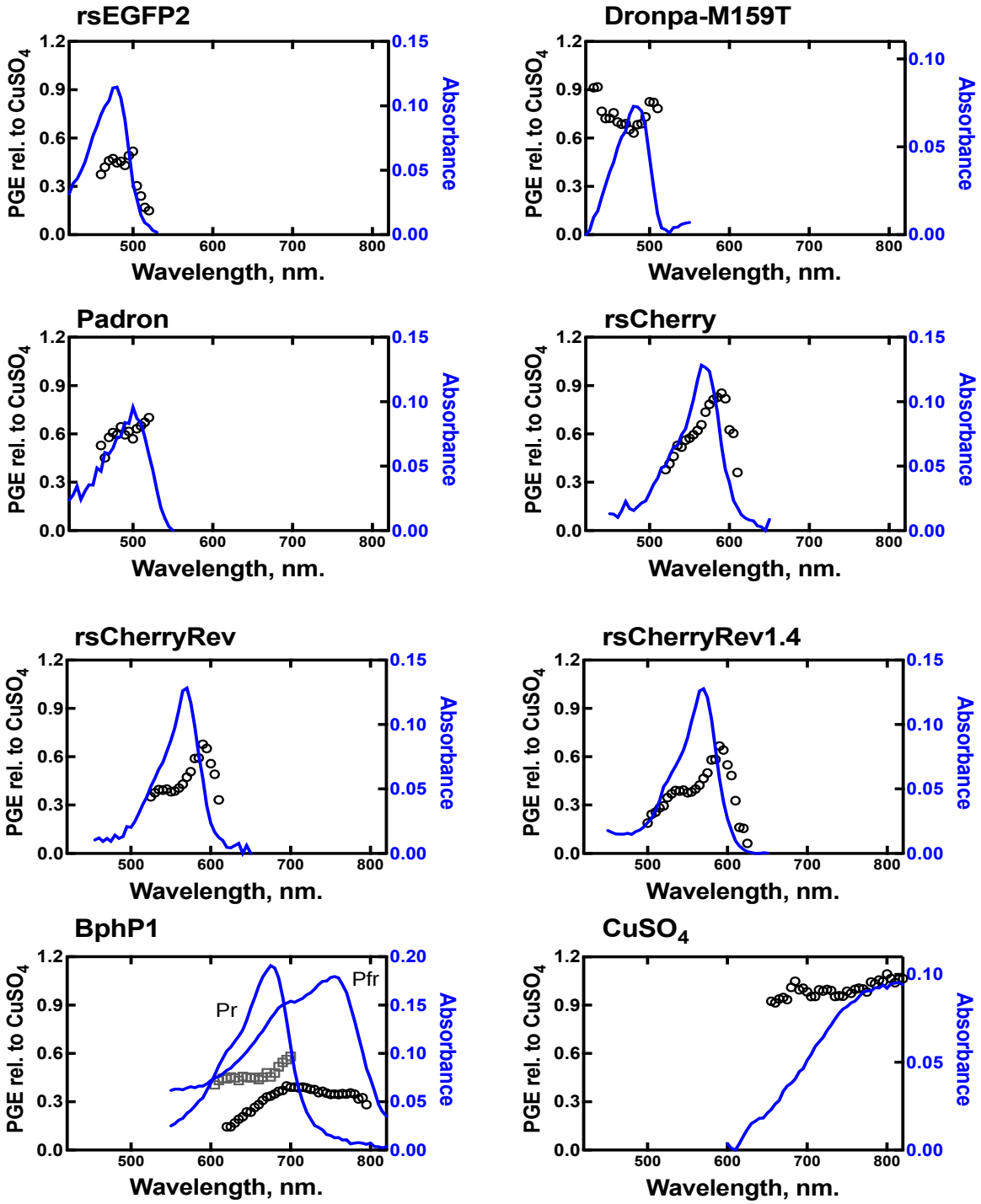

Figure S9. PGE of selected proteins as a function of wavelength. PGEs have been measured in reference to copper sulfate.

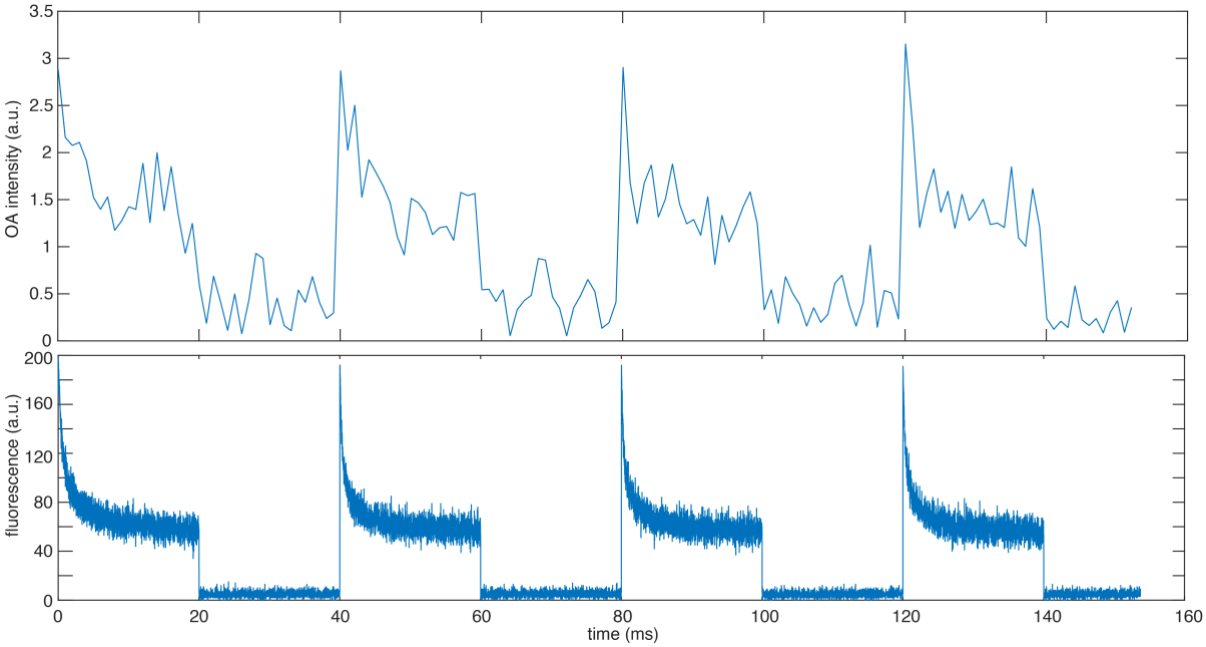

Figure S10. OA (top) and fluorescence signal trace (bottom) of rsEGFP2 switched with 20 MHz repetition rate. See method section for details.

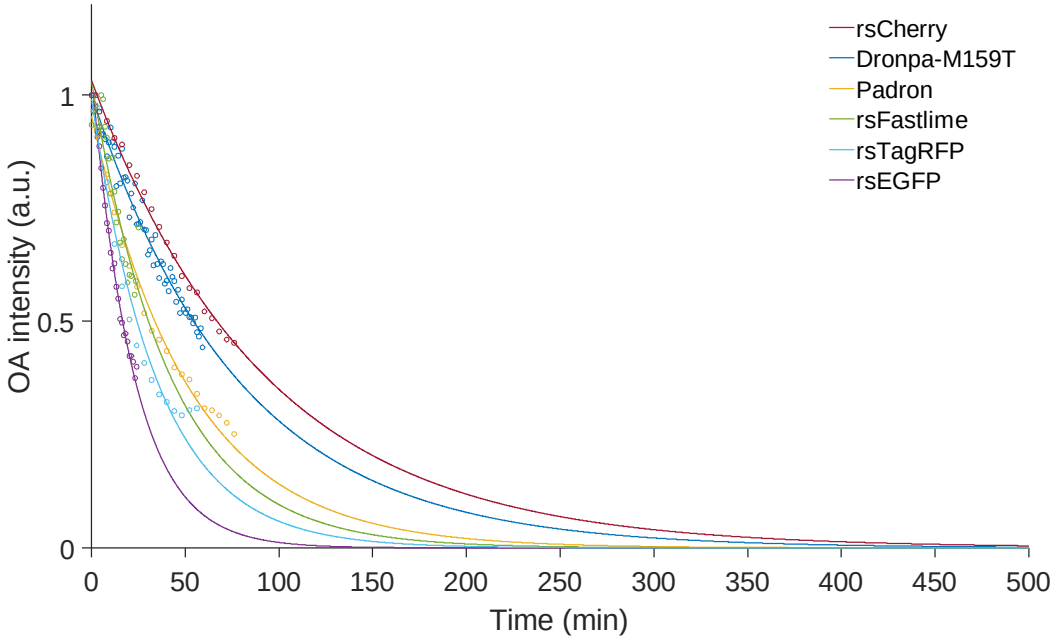

Figure S11. Bleaching of the rsFP, data is extracted from the peak values of each ON cycle in Figure 3.